

# Linear, decoupled, second-order and structure-preserving scheme for Carreau fluid equations coupled with steric Poisson-Nernst-Planck model

Wenxing Zhu<sup>a</sup>, Mingyang Pan<sup>b</sup>, Dongdong He<sup>a,\*</sup>

<sup>a</sup>*School of Science and Engineering, The Chinese University of Hong Kong, Shenzhen, Shenzhen, Guangdong, 518172, P.R.China*

<sup>b</sup>*School of Science, Hebei University of Technology, Tianjin, 300401, P.R.China*

## Abstract

In this paper, to study ionic steric effects, we present a linear, decoupled, second-order accurate in time and structure-preserving scheme with finite element approximations for Carreau fluid equations coupled with steric Poisson-Nernst-Planck (SPNP) model. The logarithmic transformation for the ion concentration is used to preserve positivity property. To deal with the nonlinear coupling terms in fluid equation, a nonlocal auxiliary variable with respect to the free energy of SPNP equations and its associated ordinary differential equation are introduced. The obtained system is equivalent to the original system. The fully discrete scheme is proved to be mass conservative, positivity-preserving for ion concentration and energy dissipative at discrete level. Some numerical simulations are provided to demonstrate its stability and accuracy. Moreover, the ionic steric effects are numerically investigated.

**Keywords:** Electrokinetic flow, steric effects, Finite element method, Fully decoupled, Second-order

## 1. Introduction

Electrokinetic flow describes the motion of electrically induced fluids. The ions are transported by advection due to fluid flow, migration under an electric potential which is generated by the distribution of charged ions and diffusion driven by concentration gradients. Conversely, the flow of fluid is driven by the electric field generated by the ions. The electrokinetic phenomenon has received much attention recently due to its widely promising applications including biomedical lab-on-a-chip devices [1], capillary electrophoresis [2], battery and fuel cell technology [3, 4], desalination of water [5], microfluidic systems [6, 7].

Electrokinetic phenomenon is usually described by the Poisson-Nernst-Planck (PNP) equations for ion transport coupled to the Navier-Stokes (NS) equations for the Newtonian fluid flow. The conventional PNP model [8, 9, 10, 11, 12] treats ions as point charges and neglects the steric effects of ions arising from their finite size. While valid for bulk or diluted solvents, this assumption could be problematic in a narrow channel pore with crowded ionic populations. Within the PNP framework, there has been a growing interest in incorporating steric effects [13, 14, 15, 16, 17, 18]. Currently, most studies on electrokinetic flow mainly rely on the Newtonian fluid flow [19, 20, 21, 22, 23, 24, 25, 26, 27], which fails to capture the shear-dependent viscosity in complex fluids. To advance modeling of electrokinetic phenomenon in rheologically complex media, we aim to investigate the dynamics of ions with finite size in non-Newtonian fluids with shear-dependent viscosity.

In this paper, we assume  $\Omega$  to be a rectangular bounded domain in  $\mathbb{R}^2$  with a Lipschitz continuous boundary  $\partial\Omega$ . The magnetic field is negligible, since the dynamic electric current is small. The fluid is assumed incompressible. Under these assumptions, the SPNP system governs the dynamics of ions with steric effects under the effect of electrical field, while the mass and momentum conservation equations describe the non-Newtonian fluid behavior. Therefore, the governing equations of Carreau fluid equations coupled with SPNP

\*Corresponding author.

Email address: hedongdong@cuhk.edu.cn (Dongdong He)

model may be written as

$$\rho \partial_t \mathbf{u} + \rho (\mathbf{u} \cdot \nabla) \mathbf{u} - \nabla \cdot \boldsymbol{\tau} + \nabla p = - \sum_i z_i c_i \nabla V, \quad (1a)$$

$$\nabla \cdot \mathbf{u} = 0, \quad (1b)$$

$$\partial_t c_i + \mathbf{u} \cdot \nabla c_i = D_i \nabla \cdot (c_i \nabla g_i), \quad (1c)$$

$$g_i = \log \frac{c_i}{c_0} + \frac{z_i e}{k_B T} V + \frac{e}{k_B T} \sum_j \omega_{ij} c_j, \quad (1d)$$

$$- \nabla \cdot (\epsilon \nabla V) = \sum_i z_i c_i, \quad (1e)$$

where  $c_i$  is the ion concentration of the  $i$ th species with  $i \in 1, \dots, N$ ,  $g_i$  is the chemical potential with respect to  $c_i$ ,  $z_i$  is the ionic valency,  $D_i$  is the diffusion constant,  $W = (\omega_{ij})_{N \times N}$  is the coefficient matrix for steric interactions,  $\omega_{ij}$  is a nonnegative constant depending on ion radii,  $k_B$  is the Boltzmann's constant,  $T$  is the absolute temperature,  $e$  is the unit charge,  $V$  is the electrostatic potential,  $\epsilon$  is the electric permittivity,  $\rho$  is the fluid density,  $\mathbf{u}$  is fluid velocity,  $p$  is the pressure,  $\boldsymbol{\tau} = 2\mu_p \mathbb{D}\mathbf{u}$  is the shear stress tensor,  $\mathbb{D}\mathbf{u} = \frac{1}{2}[\nabla \mathbf{u} + (\nabla \mathbf{u})^T]$  is the deformation tensor, and the apparent viscosity  $\mu_p$  is assumed to follow the Carreau model [28, 29, 30]:

$$\mu_p = \mu_\infty + (\mu_0 - \mu_\infty) \left( 1 + \lambda_1^2 (2\mathbb{D}\mathbf{u} : \mathbb{D}\mathbf{u}) \right)^{\frac{k-1}{2}}, \quad (2)$$

$\mu_0$  is the viscosity at zero shear rate,  $\mu_\infty$  ( $\mu_0 > \mu_\infty > 0$ ) is the viscosity at infinite shear rate,  $\lambda_1$  is the relaxation time constant,  $k$  is the power index. It can be seen from (2) that at a low shear rate, Carreau fluid behaves as a Newtonian fluid and at a high shear rate as a power law [31, 32] fluid. The Carreau model is mostly used for food, beverages and also blood flow applications. In this system (1), we assume that  $W$  is positive definite and  $D_i = D$ .

The classical Navier–Stokes–Poisson–Nernst–Planck (NSPNP) system can hardly be solved analytically due to the coupling of the velocity, the electric potential and ion concentrations. For the two separate subproblems, there are many effective methods available. The projection method [33, 34, 35, 36] can decouple the velocity and pressure for NS equations. For the PNP equations, many efficient approaches are discussed in [37, 38, 39, 40, 41, 42, 43, 44]. For NSPNP system, some numerical studies have been devoted to solving this system. Prohl et al. [45] constructed an implicit and nonlinear scheme which preserves the non-negativity of the ionic concentrations. They also considered a projection method without non-negativity preserving. Metti et al. [21] also proposed a nonlinear, first-order and unconditionally energy stable time-stepping scheme with a logarithmic transformation of the ionic concentrations. He et al. [46] proposed nonlinear schemes, which preserves the positivity and satisfies energy dissipation under certain conditions and specific spatial discretization.

Compared with classical NSPNP system, the new model (1) considers non-Newtonian viscosity and ionic steric interactions. Besides the Coulomb force term coupling the electric potential and fluid velocity and the convection term coupling ionic concentration and fluid velocity, nonlinearity is further introduced by steric effects from the last term in (1d) and nonlinear viscosity dependent on shear rate in (2). Developing efficient and structure-preserving algorithm is very challenging for this highly nonlinear coupled partial differential equation system (1). This work is inspired by scalar auxiliary variable (SAV) approach to construct the structure-preserving scheme, which has received much attention recently in [47, 48, 41, 44]. Also the fully decoupled scheme can be achieved by combining with splitting method. Based on this idea, we introduce a suitable auxiliary variable and design an ordinary differential equation to deal with the nonlinear terms involved in the equations. Meanwhile, the projection method is employed to treat the fluid equations to decouple the velocity and pressure. Using logarithm transformation for the ion concentrations, we construct a linear, decoupled and second-order accurate in time scheme for the Carreau fluid equations coupled with steric PNP system which satisfies positivity preserving, mass conservative, and energy dissipative properties.

The remainder of this paper is organized as follows. In section 2, we present the dimensionless form of system (1) and reformulate it into equivalent system based on auxiliary variable approach. The energy dissipation law of the modified system is derived. In section 3, a second-order accurate in time, linear, decoupled, and structure-preserving scheme for the reformulated system is constructed. Mass conservation, positivity

for ion concentration and energy stability of the fully discrete scheme are proved. The implementation details of the proposed scheme is also presented. In section 4, some numerical examples are given to validate the theoretical analyses and the effectiveness of the proposed methods. Finally, conclusions of the present study are given in section 5.

## 2. Carreau fluid equations coupled with steric PNP model

We first introduce the governing equations in a nondimensional form, and then present three important physical properties.

### 2.1. Non-dimensionalisation

To get a nondimensional formulation, we introduce the following dimensionless variables:

$$\begin{aligned}\tilde{\mathbf{x}} &= \frac{\mathbf{x}}{\hat{l}}, \quad \tilde{\mathbf{u}} = \frac{\mathbf{u}}{\hat{u}}, \quad \tilde{t} = \frac{t}{\hat{l}/\hat{u}}, \quad \tilde{c}_i = \frac{c_i}{c_0}, \quad \tilde{\mu}_p = \frac{\mu_p}{\hat{\mu}}, \quad \tilde{\mu}_0 = \frac{\mu_0}{\hat{\mu}} \\ \tilde{V} &= \frac{V}{k_B T/e}, \quad \tilde{p} = \frac{p}{\rho \hat{u}^2}, \quad \tilde{\omega}_{ij} = \frac{\omega_{ij} c_0 e}{k_B T}, \quad \tilde{\mu}_\infty = \frac{\mu_\infty}{\hat{\mu}}, \quad \tilde{\lambda}_1 = \lambda_1 \frac{\hat{u}}{\hat{l}}.\end{aligned}$$

For clarity, we omit all the tildes of the dimensionless variables. Then the govern equations (1) in dimensionless form become:

$$\partial_t \mathbf{u} + (\mathbf{u} \cdot \nabla) \mathbf{u} - \frac{1}{Re} \nabla \cdot (2\mu_p \mathbb{D} \mathbf{u}) + \nabla p = -Co \sum_i z_i c_i \nabla V, \quad (3a)$$

$$\nabla \cdot \mathbf{u} = 0, \quad (3b)$$

$$\partial_t c_i + \nabla \cdot (\mathbf{u} c_i) = \frac{1}{Pe} \nabla \cdot (c_i \nabla g_i), \quad (3c)$$

$$g_i = \log c_i + z_i V + \sum_j \omega_{ij} c_j, \quad (3d)$$

$$-\lambda \Delta V = \sum_i z_i c_i, \quad (3e)$$

$$\mu_p = \mu_\infty + (\mu_0 - \mu_\infty) \left( 1 + \lambda_1^2 (2\mathbb{D} \mathbf{u} : \mathbb{D} \mathbf{u}) \right)^{\frac{k-1}{2}}, \quad (3f)$$

where the nondimensional numbers are defined as follows

$$Re = \frac{\rho \hat{u} \hat{l}}{\hat{\mu}}, \quad Co = \frac{c_0 k_B T}{\rho \hat{u}^2 e}, \quad Pe = \frac{\hat{l} \hat{u}}{D}, \quad \lambda = \frac{\epsilon k_B T}{\hat{l}^2 c_0 e}.$$

Here,  $Re$  is the Reynolds number,  $Co$  is the Coulomb-driven number,  $Pe$  is the Péclet number, and  $\lambda$  is the ratio of Debye length to the characteristic length. The initial conditions and boundary conditions are given by

$$c_i|_{t=0} = c_{i0}, \quad -\lambda \Delta V|_{t=0} = \sum_i z_i c_{i0}, \quad \mathbf{u}|_{t=0} = \mathbf{u}_0, \quad (4)$$

$$\frac{\partial c_i}{\partial \mathbf{n}}|_{\partial \Omega} = 0, \quad \frac{\partial V}{\partial \mathbf{n}}|_{\partial \Omega} = 0, \quad \mathbf{u}|_{\partial \Omega} = \mathbf{0}, \quad (5)$$

where  $\mathbf{n}$  is the unit outward normal on the boundary  $\partial \Omega$ . Note that the electrostatic potential  $V$  and pressure  $p$  are determined up to a constant, we select unique solutions  $V, p$  by requiring

$$\int_{\Omega} V d\mathbf{x} = 0, \quad \int_{\Omega} p d\mathbf{x} = 0.$$

The total free energy of (3) is defined as:

$$E = E_{\mathbf{u}} + E_V + E_{ent} + E_{ster}, \quad (6)$$

where kinetic energy  $E_u$ , electric field energy  $E_V$ , entropic contribution  $E_{ent}$ , and steric interaction energy  $E_{ster}$  are given by

$$\begin{aligned} E_u &= \int_{\Omega} \frac{1}{2} |\mathbf{u}|^2 d\mathbf{x}, \\ E_V &= \int_{\Omega} \frac{1}{2} \lambda Co |\nabla V|^2 d\mathbf{x}, \\ E_{ent} &= \int_{\Omega} Co \sum_i c_i (\log c_i - 1) d\mathbf{x}, \\ E_{ster} &= \int_{\Omega} \frac{1}{2} Co \sum_i \sum_j \omega_{ij} c_i c_j d\mathbf{x}. \end{aligned}$$

## 2.2. Basic properties

We now present a few physical properties of the system (3), which play important role in designing numerical schemes.

1. Positivity: Suppose that  $c_i(\mathbf{x}, 0) > 0, \forall \mathbf{x} \in \Omega$ , then

$$c_i(\mathbf{x}, t) > 0, \quad \forall t > 0, \mathbf{x} \in \Omega.$$

The term  $\log c_i$  in (3c) must require  $c_i$  is always positive.

2. Mass conservation:

$$\int_{\Omega} c_i(\mathbf{x}, t) d\mathbf{x} = \int_{\Omega} c_i(\mathbf{x}, 0) d\mathbf{x}, \quad \forall t > 0.$$

The mass conservation can be obtained by integrating (3c) over  $\Omega$ , using the integration by parts and applying the boundary conditions (5).

3. Energy dissipation:

$$\frac{dE}{dt} \leq 0.$$

The energy dissipation law for the system (3) can be obtained by the following process. Taking the  $L^2$  inner product of (3a) with  $\mathbf{u}$ , using (3b) and integration by parts can arrive at

$$\frac{d}{dt} \int_{\Omega} \frac{1}{2} |\mathbf{u}|^2 d\mathbf{x} = (\partial_t \mathbf{u}, \mathbf{u}) = -\frac{1}{Re} \|\sqrt{2\mu_p} \mathbb{D} \mathbf{u}\|_F^2 - Co \left( \sum_i z_i c_i \nabla V, \mathbf{u} \right), \quad (7)$$

where  $\|\cdot\|_F$  is Frobenius norm. Differentiating (3e) with respect to time  $t$ , taking the  $L^2$  inner product with  $CoV$  and integrating by parts, we obtain

$$\frac{d}{dt} \int_{\Omega} \frac{Co}{2} \lambda |\nabla V|^2 d\mathbf{x} = -Co \left( (\nabla \cdot (\lambda \nabla V))_t, V \right) = Co \left( \sum_i z_i \partial_t c_i, V \right). \quad (8)$$

Taking the  $L^2$  inner product of (3c) with  $Co g_i$ , using (3d), (3b) and integration by parts, taking the summation for  $i$  to get

$$\begin{aligned} & \frac{d}{dt} \left( \int_{\Omega} \sum_i Co c_i (\log c_i - 1) d\mathbf{x} + \int_{\Omega} \frac{Co}{2} \sum_i \sum_j \omega_{ij} c_i c_j d\mathbf{x} \right) + \sum_i Co (z_i V, \partial_t c_i) \\ &= - \sum_i Co \int_{\Omega} \nabla \cdot (\mathbf{u} c_i) (\log c_i + z_i V + \sum_j \omega_{ij} c_j) d\mathbf{x} - \frac{Co}{Pe} \sum_i \int_{\Omega} c_i |\nabla g_i|^2 d\mathbf{x} \\ &= \sum_i Co \left( \int_{\Omega} \mathbf{u} \cdot \nabla c_i d\mathbf{x} + \int_{\Omega} z_i c_i \mathbf{u} \cdot \nabla V d\mathbf{x} + \int_{\Omega} \mathbf{u} \cdot \nabla \left( \frac{1}{2} \sum_j \omega_{ij} c_i c_j \right) d\mathbf{x} - \frac{1}{Pe} \int_{\Omega} c_i |\nabla g_i|^2 d\mathbf{x} \right) \\ &= \int_{\Omega} \sum_i Co z_i c_i \mathbf{u} \cdot \nabla V d\mathbf{x} - \frac{Co}{Pe} \sum_i \int_{\Omega} c_i |\nabla g_i|^2 d\mathbf{x}. \end{aligned} \quad (9)$$



Combining (8) and (9), we have

$$\frac{d}{dt}(E_{ent} + E_{ster} + E_V) = -\frac{Co}{Pe} \sum_i \int_{\Omega} c_i |\nabla g_i|^2 d\mathbf{x} + \int_{\Omega} \sum_i Co z_i c_i \mathbf{u} \cdot \nabla V d\mathbf{x}, \quad (10)$$

From (7) and (10), the obtained energy law reads as follows:

$$\frac{dE}{dt} = -\frac{Co}{Pe} \sum_i \int_{\Omega} c_i |\nabla g_i|^2 d\mathbf{x} - \frac{1}{Re} \|\sqrt{2\mu_p} \mathbb{D}\mathbf{u}\|_F^2 \leq 0. \quad (11)$$

### 2.3. Reformulation

To preserve the positivity of the ion concentration, we consider the logarithm transformation  $c_i = \exp(\sigma_i)$ . Then the evolution of  $\sigma_i$  is given by

$$\begin{aligned} \partial_t \sigma_i + \mathbf{u} \cdot \nabla \sigma_i &= \frac{1}{Pe} \left[ |\nabla \sigma_i|^2 + \Delta \sigma_i + z_i \Delta V + z_i \nabla \sigma_i \cdot \nabla V \right. \\ &\quad \left. + \sum_j \omega_{ij} \nabla \sigma_i \cdot \nabla \sigma_j c_j + \sum_j \omega_{ij} |\nabla \sigma_j|^2 c_j + \sum_j \omega_{ij} \Delta \sigma_j c_j \right]. \end{aligned} \quad (12)$$

Next, to construct a decoupling and energy stable scheme, we introduce a nonlocal variable  $r(t)$  such that

$$r(t) = \sqrt{E_{SPNP} + B}, \quad (13)$$

where  $E_{SPNP} = E_{ent} + E_{ster} + E_V$ ,  $B$  is a positive constant to guarantee the radicand is always positive. Note that  $E_V$ ,  $E_{ent}$  and  $E_{ster}$  are convex functions, we can always find such a constant  $B$  since the summation of  $E_V$ ,  $E_{ent}$  and  $E_{ster}$  are bounded from below. Then we define a nonlocal variable  $\xi(t)$  such that

$$\xi(t) = \frac{r}{\sqrt{E_{SPNP} + B}}.$$

It is easy to see that  $\xi(t) = 1$ . Differentiating (13) with respect to time  $t$ , using (10), adding the zero-valued term  $\int_{\Omega} (\mathbf{u} \cdot \nabla) \mathbf{u} \cdot \mathbf{u} d\mathbf{x}$  and multiplying by the factor  $\xi(t)$ , the associated ordinary differential equation is

$$\frac{dr}{dt} = \frac{1}{2\sqrt{E_{SPNP} + B}} \left( -\frac{Co}{Pe} \xi \sum_i \int_{\Omega} c_i |\nabla g_i|^2 d\mathbf{x} + \int_{\Omega} \sum_i Co z_i c_i \mathbf{u} \cdot \nabla V d\mathbf{x} + \int_{\Omega} (\mathbf{u} \cdot \nabla) \mathbf{u} \cdot \mathbf{u} d\mathbf{x} \right). \quad (14)$$

Then by combining the nonlocal variables  $r(t)$ ,  $\xi(t)$  and the evolution (14), the system (3) is reformulated to the following form:

$$\partial_t \mathbf{u} + \xi(\mathbf{u} \cdot \nabla) \mathbf{u} - \frac{1}{Re} \nabla \cdot (2\mu_p \mathbb{D}\mathbf{u}) + \nabla p = -Co\xi \sum_i z_i c_i \nabla V, \quad (15a)$$

$$\nabla \cdot \mathbf{u} = 0, \quad (15b)$$

$$c_i = \exp(\sigma_i), \quad (15c)$$

$$\begin{aligned} \partial_t \sigma_i + \mathbf{u} \cdot \nabla \sigma_i &= \frac{1}{Pe} \left[ |\nabla \sigma_i|^2 + \Delta \sigma_i + z_i \Delta V + z_i \nabla \sigma_i \cdot \nabla V \right. \\ &\quad \left. + \sum_j \omega_{ij} \nabla \sigma_i \cdot \nabla \sigma_j c_j + \sum_j \omega_{ij} |\nabla \sigma_j|^2 c_j + \sum_j \omega_{ij} \Delta \sigma_j c_j \right], \end{aligned} \quad (15d)$$

$$-\lambda \Delta \bar{V} = \sum_i z_i c_i, \quad (15e)$$

$$V = \xi \bar{V}, \quad (15f)$$

$$\begin{aligned} \frac{dr}{dt} &= \frac{1}{2\sqrt{E_{SPNP} + B}} \left( -\frac{Co}{Pe} \xi \sum_i \int_{\Omega} c_i |\nabla g_i|^2 d\mathbf{x} \right. \\ &\quad \left. + \int_{\Omega} \sum_i Co z_i c_i \mathbf{u} \cdot \nabla V d\mathbf{x} + \int_{\Omega} (\mathbf{u} \cdot \nabla) \mathbf{u} \cdot \mathbf{u} d\mathbf{x} \right), \end{aligned} \quad (15g)$$

$$\mu_p = \mu_{\infty} + (\mu_0 - \mu_{\infty}) \left( 1 + \lambda_1^2 (2\mathbb{D}\mathbf{u} : \mathbb{D}\mathbf{u}) \right)^{\frac{k-1}{2}}. \quad (15h)$$

The transformed system (19) satisfies the following initial conditions:

$$\begin{aligned} c_i|_{t=0} &= c_{i0}, \quad -\lambda \Delta V|_{t=0} = \sum_i z_i c_{i0}, \quad \mathbf{u}|_{t=0} = \mathbf{u}_0, \\ r|_{t=0} &= \sqrt{\int_{\Omega} \frac{1}{2} \lambda Co |\nabla V_0|^2 d\mathbf{x} + Co \int_{\Omega} \sum_i c_{i0} (\log c_{i0} - 1) d\mathbf{x} + \int_{\Omega} \frac{1}{2} Co \sum_i \sum_j \omega_{ij} c_{i0} c_{j0} d\mathbf{x} + B}. \end{aligned}$$

Note that the new system (19) is equivalent to the original PDE system (3). Also, the new system (19) follows an energy dissipative law. Taking the  $L^2$  inner product of (15a) with  $\mathbf{u}$ , using (15b) and integration by parts, we obtain

$$\frac{d}{dt} \int_{\Omega} \frac{1}{2} |\mathbf{u}|^2 d\mathbf{x} = -\frac{1}{Re} \|\sqrt{2\mu_p} \mathbb{D}\mathbf{u}\|_F^2 - Co \xi \left( \sum_i z_i c_i \nabla V, \mathbf{u} \right). \quad (16)$$

By multiplying (15g) with  $2r$ , we obtain

$$\frac{dr^2}{dt} = -\frac{Co}{Pe} |\xi|^2 \sum_i \int_{\Omega} c_i |\nabla g_i|^2 d\mathbf{x} + Co \xi \int_{\Omega} \sum_i z_i c_i \mathbf{u} \cdot \nabla V d\mathbf{x}. \quad (17)$$

Combining (16) and (17), the obtained energy law in the new form can read as:

$$\frac{d}{dt} \left( \int_{\Omega} \frac{1}{2} |\mathbf{u}|^2 d\mathbf{x} + r^2 - B \right) = -\frac{Co}{Pe} |\xi|^2 \sum_i \int_{\Omega} c_i |\nabla g_i|^2 d\mathbf{x} - \frac{1}{Re} \|\sqrt{2\mu_p} \mathbb{D}\mathbf{u}\|_F^2. \quad (18)$$

### 3. Full discrete scheme

Let  $0 < h < 1$  denote the mesh size and  $\mathcal{T}_h$  be a uniform partition of  $\bar{\Omega} = \cup_{K \in \mathcal{T}_h} K$  into non-overlapping triangles. Given a  $\mathcal{T}_h$ , we consider the following finite element space

$$\begin{aligned} X_h &= \{ \mathbf{v}_h \in H_0^1(\Omega)^2 \cap C^0(\bar{\Omega})^2 : v_{h|K} \in P_{l_1}(K), \forall K \in \mathcal{T}_h \}, \\ M_h &= \{ q_h \in L_0^2(\Omega) \cap C^0(\bar{\Omega}) : q_{h|K} \in P_{l_2}(K), \forall K \in \mathcal{T}_h \}, \\ Q_h &= \{ \varphi_h \in H^1(\Omega) \cap C^0(\bar{\Omega}) : \varphi_{h|K} \in P_{l_3}(K), \forall K \in \mathcal{T}_h \}, \\ S_h &= Q_h \cap L_0^2(\Omega), \end{aligned}$$

where  $P_{l_m}$  is the space of piecewise polynomials of total degree no more than  $l_m$ ,  $L_0^2(\Omega) = \{ q \in L^2(\Omega) : \int_{\Omega} q dx = 0 \}$  and  $H_0^1(\Omega) = \{ s \in H^1(\Omega) : s = 0 \text{ on } \partial\Omega \}$ . Additionally, assume that the finite element spaces  $(X_h, M_h)$  satisfy the discrete inf-sup inequality [49]: for each  $q_h \in M_h$ , there exists a positive constant  $\beta > 0$  such that

$$\sup_{\mathbf{v}_h \in X_h, \mathbf{v}_h \neq 0} \frac{(q_h, \nabla \cdot \mathbf{v}_h)}{\|\nabla \mathbf{v}_h\|_0} \geq \beta \|q_h\|_0.$$

To discrete (19) in space by using finite element method, we first write variational formulations for (19) which reads as: find  $(\sigma, c_i, V, \bar{V}, \mathbf{u}, p) \in H^1(\Omega) \times H^1(\Omega) \times (H^1(\Omega) \cap L_0^2(\Omega)) \times (H^1(\Omega) \cap L_0^2(\Omega)) \times H_0^1(\Omega)^2 \times L_0^2(\Omega)$

such that for all  $(\eta_i, \phi, \mathbf{v}, q) \in H^1(\Omega) \times H^1(\Omega) \times H_0^1(\Omega)^2 \times L_0^2(\Omega)$ ,

$$(\partial_t \mathbf{u}, \mathbf{v}) + (\xi(\mathbf{u} \cdot \nabla) \mathbf{u}, \mathbf{v}) + \frac{1}{Re} (2\mu_p \mathbb{D} \mathbf{u}, \mathbb{D} \mathbf{v}) + (\nabla p, \mathbf{v}) = -Co \left( \sum_i z_i c_i \nabla V, \mathbf{v} \right) \quad (19a)$$

$$(\nabla \cdot \mathbf{u}, q) = 0, \quad (19b)$$

$$c_i = \exp(\eta_i), \quad (19c)$$

$$\begin{aligned} (\partial_t \sigma_i, \eta_i) + (\mathbf{u} \cdot \nabla \sigma_i, \eta_i) &= \frac{1}{Pe} \left[ (|\nabla \sigma_i|^2, \eta_i) - (\nabla \sigma_i, \nabla \eta_i) - z_i (\nabla V, \nabla \eta_i) \right. \\ &\quad \left. + z_i (\nabla \sigma_i \cdot \nabla V, \eta_i) + \sum_j (\omega_{ij} \nabla \sigma_i \cdot \nabla \sigma_j c_j, \eta_i) - \sum_j \omega_{ij} \nabla \sigma_j c_j, \nabla \eta_i \right], \end{aligned} \quad (19d)$$

$$\lambda (\nabla \bar{V}, \nabla \phi) = \sum_i (z_i c_i, \phi), \quad (19e)$$

$$\xi = \frac{r}{\sqrt{E_{SPNP} + B}}, \quad (19f)$$

$$V = \xi \bar{V}, \quad (19g)$$

$$\begin{aligned} \frac{dr}{dt} &= \frac{1}{2\sqrt{E_{SPNP} + B}} \left( -\frac{Co}{Pe} \xi \sum_i \int_{\Omega} c_i |\nabla g_i|^2 d\mathbf{x} \right. \\ &\quad \left. + \int_{\Omega} \sum_i Co z_i c_i \mathbf{u} \cdot \nabla V d\mathbf{x} + \int_{\Omega} (\mathbf{u} \cdot \nabla) \mathbf{u} \cdot \mathbf{u} d\mathbf{x} \right), \end{aligned} \quad (19h)$$

$$\mu_p = \mu_{\infty} + (\mu_0 - \mu_{\infty}) \left( 1 + \lambda^2 (2\mathbb{D} \mathbf{u} : \mathbb{D} \mathbf{u}) \right)^{\frac{k-1}{2}}. \quad (19i)$$

### 3.1. Numerical scheme

We discretize the system (19) in space by finite element method and in time by second-order backward differentiation formula, leading to the fully discrete second-order scheme: find  $(\sigma_{ih}^{n+1}, \bar{c}_{ih}^{n+1}, c_{ih}^{n+1}, \bar{V}_h^{n+1}, V_h^{n+1}, \mathbf{u}_h^{n+1})$ ,

$p_h^{n+1}) \in (Q_h, Q_h, Q_h, S_h, S_h, X_h, M_h)$ , such that for all  $(\eta_{ih}, \phi_h, \mathbf{v}_h, q_h) \in (Q_h, Q_h, X_h, M_h)$

$$\begin{aligned} & \left( \frac{3\tilde{\mathbf{u}}_h^{n+1} - 4\mathbf{u}_h^n + \mathbf{u}_h^{n-1}}{2\Delta t}, \mathbf{v}_h \right) + \xi^{n+1}((\mathbf{u}_h^* \cdot \nabla)\mathbf{u}_h^*, \mathbf{v}_h) + \frac{1}{Re}(2\mu_{ph}^* \mathbb{D}\tilde{\mathbf{u}}_h^{n+1}, \mathbb{D}\mathbf{v}_h) \\ & + (\nabla p_h^n, \mathbf{v}_h) = -Co\xi^{n+1} \left( \sum_i z_i c_{ih}^{n+1} \nabla \bar{V}_h^{n+1}, \mathbf{v}_h \right), \end{aligned} \quad (20a)$$

$$(\nabla \psi_h^{n+1}, \nabla q_h) = \frac{3}{2\Delta t}(\tilde{\mathbf{u}}_h^{n+1}, \nabla q_h), \quad (20b)$$

$$\mathbf{u}_h^{n+1} = \tilde{\mathbf{u}}_h^{n+1} - \frac{2\Delta t}{3} \nabla \psi_h^{n+1}, \quad (20c)$$

$$p_h^{n+1} = \psi_h^{n+1} + p_h^n, \quad (20d)$$

$$\begin{aligned} & \left( \frac{3\sigma_{ih}^{n+1} - 4\sigma_{ih}^n + \sigma_{ih}^{n-1}}{2\Delta t}, \eta_{ih} \right) + (\mathbf{u}_h^* \cdot \nabla \sigma_{ih}^{n+1}, \eta_{ih}) + (\nabla \sigma_{ih}^{n+1}, \nabla \eta_{ih}) \\ & = \frac{1}{Pe} \left( (\nabla \sigma_{ih}^* \cdot \nabla \sigma_{ih}^{n+1}, \eta_{ih}) - z_i (\nabla V_h^*, \nabla \eta_i) + (z_i \nabla \sigma_{ih}^{n+1} \cdot \nabla V_h^*, \eta_{ih}) \right. \\ & \quad \left. + \left( \sum_j \omega_{ij} \nabla \sigma_{ih}^{n+1} \cdot \nabla \sigma_{jh}^* c_{jh}^*, \eta_{ih} \right) - (\omega_{ij} \nabla \sigma_{jh}^* c_{jh}^*, \nabla \eta_{ih}) - (\omega_{ij} \nabla \sigma_{ih}^{n+1} c_{ih}^*, \nabla \eta_{ih}) \right), \end{aligned} \quad (20e)$$

$$\bar{c}_{ih}^{n+1} = \exp(\sigma_{ih}^{n+1}), \quad (20f)$$

$$c_{ih}^{n+1} = \frac{(c_{ih}^n, 1)}{(\bar{c}_{ih}^{n+1}, 1)} \bar{c}_{ih}^{n+1}, \quad (20g)$$

$$(\lambda \nabla \bar{V}_h^{n+1}, \nabla \phi_h) = \sum_i (z_i c_{ih}^{n+1}, \phi_h), \quad (20h)$$

$$V_h^{n+1} = \xi^{n+1} \bar{V}_h^{n+1}, \quad (20i)$$

$$\xi^{n+1} = \frac{r^{n+1}}{\sqrt{\bar{E}_{SPNP}^{n+1} + B}}, \quad (20j)$$

$$\begin{aligned} & \frac{3r^{n+1} - 4r^n + r^{n-1}}{2\Delta t} = \frac{1}{2\sqrt{\bar{E}_{SPNP}^{n+1} + B}} \left( -\frac{Co}{Pe} \xi^{n+1} \sum_i \|\sqrt{c_{ih}^{n+1}} \nabla \bar{g}_{ih}^{n+1}\|^2 \right. \\ & \quad \left. + Co \left( \sum_i z_i c_{ih}^{n+1} \tilde{\mathbf{u}}_h^{n+1}, \nabla \bar{V}_h^{n+1} \right) + ((\mathbf{u}_h^* \cdot \nabla) \mathbf{u}_h^*, \tilde{\mathbf{u}}_h^{n+1}) \right), \end{aligned} \quad (20k)$$

$$\mu_{ph}^{n+1} = \mu_\infty + (\mu_0 - \mu_\infty) \left( 1 + \lambda_1^2 (2\mathbb{D}\mathbf{u}_h^{n+1} : \mathbb{D}\mathbf{u}_h^{n+1}) \right)^{\frac{k-1}{2}}. \quad (20l)$$

where

$$\begin{aligned} \mathbf{u}_h^* &= 2\mathbf{u}_h^n - \mathbf{u}_h^{n-1}, \quad \bar{g}_{ih}^{n+1} = \log c_{ih}^{n+1} + z_i \bar{V}_h^{n+1} + \sum_j \omega_{ij} c_{jh}^{n+1}, \\ \sigma_{ih}^* &= 2\sigma_{ih}^n - \sigma_{ih}^{n-1}, \quad c_{ih}^* = 2c_{ih}^n - c_{ih}^{n-1}, \quad \mu_{ph}^* = 2\mu_{ph}^n - \mu_{ph}^{n-1}, \\ \bar{E}_{SPNP}^{n+1} &= \frac{\lambda Co}{2} \|\nabla \bar{V}_h^{n+1}\|^2 + Co \sum_i (c_{ih}^{n+1}, \log c_{ih}^{n+1} - 1) + \frac{Co}{2} \sum_i \sum_j \omega_{ij} (c_{ih}^{n+1}, c_{jh}^{n+1}). \end{aligned}$$

**Theorem 3.1.** *The fully discrete scheme (20) satisfies the following properties:*

1. *Positivity preservation:*  $c_{ih}^{n+1} > 0$ .
2. *Mass conservation:*

$$(c_{ih}^n, 1) = (c_{ih}^{n+1}, 1).$$

3. *Energy dissipation:*

$$\frac{E_h^{n+1} - E_h^n}{\Delta t} \leq -\frac{1}{Re} \|\sqrt{2\mu_{ph}^*} \mathbb{D}\tilde{\mathbf{u}}_h^{n+1}\|_F^2 - |\xi^{n+1}|^2 \frac{Co}{Pe} \sum_i \|\sqrt{c_{ih}^{n+1}} \nabla \bar{g}_{ih}^{n+1}\|^2, \quad (21)$$

where

$$E_h^{n+1} = \frac{1}{2} \left( \frac{1}{2} \|\mathbf{u}_h^{n+1}\|^2 + \frac{1}{2} \|2\mathbf{u}_h^{n+1} - \mathbf{u}_h^n\|^2 \right) + \frac{\Delta t^2}{3} \|\nabla p_h^{n+1}\|^2 + \frac{1}{2} (|r^{n+1}|^2 + |2r^{n+1} - r^n|^2).$$

*Proof.* First, we prove the positivity preserving. It is easy to see that  $\bar{c}_{ih}^{n+1} > 0$  from (20f) and  $c_{ih}^n > 0$  from positivity of the ion concentration at the previous step. Thus we can arrive at

$$(\bar{c}_{ih}^{n+1}, 1) > 0, \quad (c_{ih}^n, 1) > 0.$$

By (20g), we have  $c_{ih}^{n+1} > 0$ .

Next, the mass conservation can be obtained by taking the  $L^2$  inner product with the constant function 1 on both sides of the equation (20g).

It remains to prove the energy dissipation. Taking  $\mathbf{v}_h = 2\Delta t \tilde{\mathbf{u}}_h^{n+1}$  in (20a), we have

$$\begin{aligned} & (3\tilde{\mathbf{u}}_h^{n+1} - 4\mathbf{u}_h^n + \mathbf{u}_h^{n-1}, \tilde{\mathbf{u}}_h^{n+1}) + 2\Delta t \xi^{n+1} ((\mathbf{u}_h^* \cdot \nabla) \mathbf{u}_h^*, \tilde{\mathbf{u}}_h^{n+1}) + 2\Delta t (\nabla p_h^n, \tilde{\mathbf{u}}_h^{n+1}) \\ & = -2\Delta t Co \xi^{n+1} \left( \sum_i z_i c_{ih}^{n+1} \nabla \bar{V}_h^{n+1}, \tilde{\mathbf{u}}_h^{n+1} \right) - \frac{2\Delta t}{Re} \|\sqrt{2\mu_{ph}^*} \mathbb{D} \tilde{\mathbf{u}}_h^{n+1}\|_F^2. \end{aligned} \quad (22)$$

From (20b) - (20d), we have

$$(\mathbf{u}_h^{n+1}, \nabla q_h) = 0, \quad (23)$$

$$(\mathbf{u}_h^{n+1}, \tilde{\mathbf{u}}_h^{n+1} - \mathbf{u}_h^{n+1}) = \left( \mathbf{u}_h^{n+1}, \frac{2\Delta t}{3} \nabla (p_h^{n+1} - p_h^n) \right) = 0. \quad (24)$$

It follows from (20b) and (20d) that

$$\frac{\sqrt{3}}{\sqrt{2}} \mathbf{u}_h^{n+1} + \frac{\sqrt{2}}{\sqrt{3}} \Delta t \nabla p_h^{n+1} = \frac{\sqrt{3}}{\sqrt{2}} \tilde{\mathbf{u}}_h^{n+1} + \frac{\sqrt{2}}{\sqrt{3}} \Delta t \nabla p_h^n.$$

By taking the discrete inner product of the above equality with itself on both sides and using (23), we get

$$\frac{3}{2} \|\mathbf{u}_h^{n+1}\|^2 + \frac{2}{3} (\Delta t)^2 \|\nabla p_h^{n+1}\|^2 = \frac{3}{2} \|\tilde{\mathbf{u}}_h^{n+1}\|^2 + \frac{2}{3} (\Delta t)^2 \|\nabla p_h^n\|^2 + 2\Delta t (\nabla p_h^n, \tilde{\mathbf{u}}_h^{n+1}). \quad (25)$$

Using (24) and the following identity

$$2(a-b)a = |a|^2 - |b|^2 + |a-b|^2, \quad (26)$$

$$2(3a-4b+c)a = |a|^2 + |2a-b|^2 - |b|^2 - |2b-c|^2 + |a-2b+c|^2, \quad (27)$$

we have

$$\begin{aligned} & (3\tilde{\mathbf{u}}_h^{n+1} - 4\mathbf{u}_h^n + \mathbf{u}_h^{n-1}, \tilde{\mathbf{u}}_h^{n+1}) = (3(\tilde{\mathbf{u}}_h^{n+1} - \mathbf{u}_h^{n+1}) + 3\mathbf{u}_h^{n+1} - 4\mathbf{u}_h^n + \mathbf{u}_h^{n-1}, \tilde{\mathbf{u}}_h^{n+1}) \\ & = 3(\tilde{\mathbf{u}}_h^{n+1} - \mathbf{u}_h^{n+1}, \tilde{\mathbf{u}}_h^{n+1}) + (3\mathbf{u}_h^{n+1} - 4\mathbf{u}_h^n + \mathbf{u}_h^{n-1}, \mathbf{u}_h^{n+1}) + (3\mathbf{u}_h^{n+1} - 4\mathbf{u}_h^n + \mathbf{u}_h^{n-1}, \tilde{\mathbf{u}}_h^{n+1} - \mathbf{u}_h^{n+1}) \\ & = \frac{3}{2} (\|\tilde{\mathbf{u}}_h^{n+1}\|^2 - \|\mathbf{u}_h^{n+1}\|^2 + \|\tilde{\mathbf{u}}_h^{n+1} - \mathbf{u}_h^{n+1}\|^2) + \frac{1}{2} (\|\mathbf{u}_h^{n+1}\|^2 + \|2\mathbf{u}_h^{n+1} - \mathbf{u}_h^n\|^2 - \|\mathbf{u}_h^n\|^2 \\ & \quad - \|2\mathbf{u}_h^n - \mathbf{u}_h^{n-1}\|^2 + \|\mathbf{u}_h^{n+1} - 2\mathbf{u}_h^n + \mathbf{u}_h^{n-1}\|^2) \end{aligned} \quad (28)$$

By multiplying (20k) with  $4\Delta t r^{n+1}$  and using (26), we obtain

$$\begin{aligned} & |r^{n+1}|^2 + |2r^{n+1} - r^n|^2 - |r^n|^2 - |2r^n - r^{n-1}|^2 + |r^{n+1} - 2r^n + r^{n-1}|^2 \\ & = 2\Delta t \xi^{n+1} \left( -\frac{Co}{Pe} \xi^{n+1} \sum_i \|\sqrt{c_{ih}^{n+1}} \nabla g_{ih}^{n+1}\|^2 + Co \left( \sum_i z_i c_{ih}^{n+1} \tilde{\mathbf{u}}_h^{n+1}, \nabla \bar{V}_h^{n+1} \right) + ((\mathbf{u}_h^* \cdot \nabla) \mathbf{u}_h^*, \tilde{\mathbf{u}}_h^{n+1}) \right). \end{aligned} \quad (29)$$

Combining (22),(25),(28) and (29), we arrive at

$$\begin{aligned}
& \frac{1}{2} \left( \|\mathbf{u}_h^{n+1}\|^2 + \|2\mathbf{u}_h^{n+1} - \mathbf{u}_h^n\|^2 - \|\mathbf{u}_h^n\|^2 - \|2\mathbf{u}_h^n - \mathbf{u}_h^{n-1}\|^2 + \|\mathbf{u}_h^{n+1} - 2\mathbf{u}_h^n + \mathbf{u}_h^{n-1}\|^2 \right) \\
& + \frac{2\Delta t^2}{3} (\|\nabla p_h^{n+1}\|^2 - \|\nabla p_h^n\|^2) + \frac{3}{2} \|\mathbf{u}_h^{n+1} - \tilde{\mathbf{u}}_h^{n+1}\|^2 + |r^{n+1}|^2 + |2r^{n+1} - r^n|^2 - |r^n|^2 \\
& - |2r^n - r^{n-1}|^2 + |r^{n+1} - 2r^n + r^{n-1}|^2 = -\frac{2\Delta t}{Re} \|\sqrt{2\mu_{ph}^*} \mathbb{D} \tilde{\mathbf{u}}_h^{n+1}\|_F^2 \\
& - 2\Delta t |\xi^{n+1}|^2 \frac{Co}{Pe} \sum_i \|\sqrt{c_{ih}^{n+1}} \nabla g_{ih}^{n+1}\|^2.
\end{aligned} \tag{30}$$

Finally, we can obtain (21) from (30).  $\square$

### 3.2. Implementation

It seems that the developed scheme is not a fully decoupled scheme. Any direct iterative methods needs much time consumptions. Therefore, we using split technique to eliminate all nonlocal terms and obtain a fully decoupled implementation.

**Step 1.** Find  $\sigma_{ih}^{n+1} \in Q_h$  such that

$$\begin{aligned}
& \left( \frac{3\sigma_{ih}^{n+1} - 4\sigma_{ih}^n + \sigma_{ih}^{n-1}}{2\Delta t}, \eta_{ih} \right) + (\mathbf{u}_h^* \cdot \nabla \sigma_{ih}^{n+1}, \eta_{ih}) + (\nabla \sigma_{ih}^{n+1}, \nabla \eta_{ih}) \\
& = \frac{1}{Pe} \left( (\nabla \sigma_{ih}^* \cdot \nabla \sigma_{ih}^{n+1}, \eta_{ih}) - z_i (\nabla V_h^*, \nabla \eta_i) + (z_i \nabla \sigma_{ih}^{n+1} \cdot \nabla V_h^*, \eta_{ih}) \right. \\
& \left. + \left( \sum_j \omega_{ij} \nabla \sigma_{ih}^{n+1} \cdot \nabla \sigma_{jh}^* c_{jh}^*, \eta_{ih} \right) - (\omega_{ij} \nabla \sigma_{jh}^* c_{jh}^*, \nabla \eta_{ih}) - (\omega_{ii} \nabla \sigma_{ih}^{n+1} c_{ih}^*, \nabla \eta_{ih}) \right), \quad \forall \eta_i \in Q_h.
\end{aligned} \tag{31}$$

**Step 2.** Compute  $c_{ih}^{n+1}$  by

$$\begin{aligned}
\bar{c}_{ih}^{n+1} &= \exp(\sigma_{ih}^{n+1}), \\
c_{ih}^{n+1} &= \frac{(c_{ih}^n, 1)}{(\bar{c}_{ih}^{n+1}, 1)} \bar{c}_{ih}^{n+1}.
\end{aligned}$$

**Step 3.** Find  $\bar{V}_h^{n+1} \in S_h$  such that

$$(\lambda \nabla \bar{V}_h^{n+1}, \nabla \phi_h) = \sum_i (z_i c_{ih}^{n+1}, \phi_h), \quad \forall \phi_h \in Q_h. \tag{32}$$

**Step 4.** Find  $\tilde{\mathbf{u}}_{1h}^{n+1}, \tilde{\mathbf{u}}_{2h}^{n+1} \in X_h$  such that

$$\left( \frac{3\tilde{\mathbf{u}}_{1h}^{n+1} - 4\mathbf{u}_h^n + \mathbf{u}_h^{n-1}}{2\Delta t}, \mathbf{v}_h \right) + \frac{1}{Re} (2\mu_{ph}^* \mathbb{D} \tilde{\mathbf{u}}_{1h}^{n+1}, \mathbb{D} \mathbf{v}_h) = (\nabla \cdot \mathbf{v}_h, p_h^n), \quad \forall \mathbf{v}_h \in X_h, \tag{33}$$

$$\left( \frac{3\tilde{\mathbf{u}}_{2h}^{n+1}}{2\Delta t}, \mathbf{v}_h \right) + \frac{1}{Re} (2\mu_{ph}^* \mathbb{D} \tilde{\mathbf{u}}_{2h}^{n+1}, \mathbb{D} \mathbf{v}_h) = -((\mathbf{u}_h^* \cdot \nabla) \mathbf{u}_h^*, \mathbf{v}_h) - \left( \sum_i Co z_i c_{ih}^{n+1} \nabla \bar{V}_h^{n+1}, \mathbf{v}_h \right), \quad \forall \mathbf{v}_h \in X_h. \tag{34}$$

The above two subequations are obtained by splitting (20a). We use the nonlocal scalar variable  $\xi^{n+1}$  to split  $\tilde{\mathbf{u}}_h^{n+1}$  into a linear combination that reads as

$$\tilde{\mathbf{u}}_h^{n+1} = \tilde{\mathbf{u}}_{1h}^{n+1} + \xi^{n+1} \tilde{\mathbf{u}}_{2h}^{n+1}. \tag{35}$$

By replacing  $\tilde{\mathbf{u}}_h^{n+1}$  in (20a), we have

$$\begin{aligned}
& \left( \frac{3(\tilde{\mathbf{u}}_{1h}^{n+1} + \xi^{n+1} \tilde{\mathbf{u}}_{2h}^{n+1}) - 4\mathbf{u}_h^n + \mathbf{u}_h^{n-1}}{2\Delta t}, \mathbf{v}_h \right) + \xi^{n+1} ((\mathbf{u}_h^* \cdot \nabla) \mathbf{u}_h^*, \mathbf{v}_h) + (\nabla p_h^n, \mathbf{v}_h) \\
& + \frac{1}{Re} (2\mu_{ph}^* \mathbb{D} (\tilde{\mathbf{u}}_{1h}^{n+1} + \xi^{n+1} \tilde{\mathbf{u}}_{2h}^{n+1}), \mathbb{D} \mathbf{v}_h) = -Co \xi^{n+1} \left( \sum_i z_i c_{ih}^{n+1} \nabla \bar{V}_h^{n+1}, \mathbf{v}_h \right).
\end{aligned} \tag{36}$$

According to  $\xi^{n+1}$ , (36) can be decomposed into two subequations (33) and (34).

**Step 5.** Compute  $\xi^{n+1}$  by

$$\xi^{n+1} = \frac{2r^n - \frac{1}{2}r^{n-1} + \Delta t\zeta_1}{\frac{3}{2}\sqrt{\bar{E}_{SPNP}^{n+1} + B} + \Delta t\zeta_2}, \quad (37)$$

where

$$\begin{aligned} \zeta_1 &= \frac{1}{2\sqrt{\bar{E}_{SPNP}^{n+1} + B}} \left( Co \left( \sum_i z_i c_{ih}^{n+1} \tilde{\mathbf{u}}_{1h}^{n+1}, \nabla \bar{V}_h^{n+1} \right) + ((\mathbf{u}_h^* \cdot \nabla) \mathbf{u}_h^*, \tilde{\mathbf{u}}_{1h}^{n+1}) \right), \\ \zeta_2 &= \frac{1}{2\sqrt{\bar{E}_{SPNP}^{n+1} + B}} \left( \frac{Co}{Pe} \sum_i \|\sqrt{c_{ih}^{n+1}} \nabla g_{ih}^{n+1}\|^2 - Co \left( \sum_i z_i c_{ih}^{n+1} \tilde{\mathbf{u}}_{2h}^{n+1}, \nabla \bar{V}_h^{n+1} \right) - ((\mathbf{u}_h^* \cdot \nabla) \mathbf{u}_h^*, \tilde{\mathbf{u}}_{2h}^{n+1}) \right). \end{aligned}$$

Formula (37) is obtained by using the split form (35) in (20k). Equation (20k) can be rewritten as

$$\begin{aligned} \frac{3\xi^{n+1} \sqrt{\bar{E}_{SPNP}^{n+1} + B} - 4r^n + r^{n-1}}{2\Delta t} &= \frac{1}{2\sqrt{\bar{E}_{SPNP}^{n+1} + B}} \left( -\frac{Co}{Pe} \xi^{n+1} \sum_i \|\sqrt{c_{ih}^{n+1}} \nabla g_{ih}^{n+1}\|^2 \right. \\ &\quad \left. + Co \left( \sum_i z_i c_{ih}^{n+1} (\tilde{\mathbf{u}}_{1h}^{n+1} + \xi^{n+1} \tilde{\mathbf{u}}_{2h}^{n+1}), \nabla \bar{V}_h^{n+1} \right) + ((\mathbf{u}_h^* \cdot \nabla) \mathbf{u}_h^*, (\tilde{\mathbf{u}}_{1h}^{n+1} + \xi^{n+1} \tilde{\mathbf{u}}_{2h}^{n+1})) \right). \end{aligned} \quad (38)$$

According to  $\xi^{n+1}$ , we can derive formula (37). Then we verify that  $\xi^{n+1}$  is solvable by showing  $\sqrt{\bar{E}_{SPNP}^{n+1} + B} + \Delta t\zeta_2 \neq 0$ . Taking  $\mathbf{v}_h = \tilde{\mathbf{u}}_{2h}^{n+1}$  in (34), we have

$$-((\mathbf{u}_h^* \cdot \nabla) \mathbf{u}_h^*, \tilde{\mathbf{u}}_{2h}^{n+1}) - Co \left( \sum_i z_i c_{ih}^{n+1} \nabla \bar{V}_h^{n+1}, \tilde{\mathbf{u}}_{2h}^{n+1} \right) = \frac{3}{2\Delta t} \|\tilde{\mathbf{u}}_{2h}^{n+1}\|^2 + \frac{1}{Re} \|\sqrt{2\mu_{ph}^*} \mathbb{D} \tilde{\mathbf{u}}_{2h}^{n+1}\|_F^2 \geq 0. \quad (39)$$

Therefore,

$$\zeta_2 = \frac{1}{2\sqrt{\bar{E}_{SPNP}^{n+1} + B}} \left( \frac{Co}{Pe} \sum_i \|\sqrt{c_{ih}^{n+1}} \nabla g_{ih}^{n+1}\|^2 + \frac{3}{2\Delta t} \|\tilde{\mathbf{u}}_{2h}^{n+1}\|^2 + \frac{1}{Re} \|\sqrt{2\mu_{ph}^*} \mathbb{D} \tilde{\mathbf{u}}_{2h}^{n+1}\|_F^2 \right) \geq 0,$$

which implies  $\sqrt{\bar{E}_{SPNP}^{n+1} + B} + \Delta t\zeta_2 \neq 0$ .

**Step 6.** Update  $r^{n+1}$ ,  $V_h^{n+1}$  and  $\tilde{\mathbf{u}}_h^{n+1}$  by

$$\begin{aligned} r^{n+1} &= \xi^{n+1} \sqrt{\bar{E}_{SPNP}^{n+1} + B}, \\ V_h^{n+1} &= \xi^{n+1} \bar{V}_h^{n+1}, \\ \tilde{\mathbf{u}}_h^{n+1} &= \tilde{\mathbf{u}}_{1h}^{n+1} + \xi^{n+1} \tilde{\mathbf{u}}_{1h}^{n+1}. \end{aligned}$$

**Step 7:** Find  $\psi^{n+1} \in M_h$  such that

$$(\nabla \psi_h^{n+1}, \nabla q_h) = \frac{3}{2\Delta t} (\tilde{\mathbf{u}}_h^{n+1}, \nabla q_h), \quad \forall \psi_h \in M_h.$$

**Step 8:** Update  $\mathbf{u}_h^{n+1}$ ,  $p_h^{n+1}$ ,  $\mu_{ph}^{n+1}$  by

$$\begin{aligned} \mathbf{u}_h^{n+1} &= \tilde{\mathbf{u}}_h^{n+1} - \frac{2\Delta t}{3} \nabla \psi_h^{n+1}, \\ p_h^{n+1} &= \psi_h^{n+1} + p_h^n, \\ \mu_{ph}^{n+1} &= \mu_\infty + (\mu_0 - \mu_\infty) \left( 1 + \lambda_1^2 (2\mathbb{D} \mathbf{u}_h^{n+1} : \mathbb{D} \mathbf{u}_h^{n+1}) \right)^{\frac{k-1}{2}}. \end{aligned}$$

## 4. Numerical results

In this section, we first implement several numerical examples to verify the convergence and energy stability of the proposed scheme (20). Then, some benchmark simulations are proposed to demonstrate the effectiveness of the scheme.

In all numerical experiments below, we set the computational domain to be a rectangular domain  $\Omega = [0, 1]^2$  and use the Taylor-Hood element  $(P_2, P_1)$  for velocity and pressure. The  $P_2$  element is also used for electric potential and ion concentrations. And we consider only two types of ions: positive ion (denoted by  $i = p$ ) and negative ion (denoted by  $i = n$ ). Correspondingly, their valence numbers  $z_i$  are set to be  $z_p = 1$  and  $z_n = -1$ , respectively. Unless otherwise specified, all boundary conditions follow the default settings (5) established in this work. The computations are performed with software Freefem ++ [50].

### 4.1. Accuracy test

The computational domain is assumed to be a rectangular region  $\Omega = [0, 1]^2$ , and the terminal time is set to be  $T = 0.5$ . We take the steric interaction coefficient matrix  $\begin{pmatrix} 2 & 1 \\ 1 & 2 \end{pmatrix}$ . The parameters in the model are set as  $\lambda = 1$ ,  $Pe = 2$ ,  $Re = 1$ ,  $Co = 5$ ,  $k = 0.5$ ,  $\mu_0 = 1.0$ ,  $\mu_\infty = 0.5$ ,  $\lambda_1 = 1$ . Assuming the exact solutions of the system (3) are given as functions

$$\begin{aligned} c_p(x, y, t) &= 1.2 + \cos(\pi x) \cos(\pi y) \exp(-t), \\ c_n(x, y, t) &= 1.2 - \cos(\pi x) \cos(\pi y) \exp(-t), \\ V(x, y, t) &= \frac{1}{\pi^2} \cos(\pi x) \cos(\pi y) \exp(-t), \\ \mathbf{u}(x, y, t) &= (\pi \sin^2(\pi x) \sin(2\pi y) \exp(-t), -\pi \sin(2\pi x) \sin^2(\pi y) \exp(-t)), \\ p(x, y, t) &= \cos(\pi x) \cos(\pi y) \exp(-t). \end{aligned} \tag{40}$$

Some source terms are added so that the above solutions can satisfy the (3). The mesh size in space is set to be  $\sqrt{2}/256$  so that it is negligible compared to the time discretization error. We use quadratic element for  $\mathbf{u}$ ,  $c_i$ ,  $V$  and linear element for  $p$ . The errors in  $L^2$  norm between the numerical solutions and the exact solutions are shown in Table 1. It is clear to see that the order of convergence in time is approximately to be second-order.

Table 1: Temporal convergence for the velocity  $\mathbf{u}$ , pressure  $p$ , concentration  $c_p$ ,  $c_n$  and electric potential  $V$  by using the  $L^2$  norm.

$N$	$\ e_u\ _2$	order	$\ e_p\ _2$	order	$\ e_{c_p}\ _2$	order
16	4.5707e-04	-	1.2785e-02	-	8.8518e-05	-
32	1.1072e-04	2.05	3.1288e-03	2.03	1.4312e-05	2.63
64	2.7404e-05	2.01	7.7970e-04	2.00	2.2599e-06	2.67
128	6.8274e-06	2.00	1.9952e-04	1.97	4.5885e-07	2.30
$N$	$\ e_{c_n}\ _2$	order	$\ e_v\ _2$	order		
16	5.2692e-05	-	7.0894e-06	-		
32	1.0068e-05	2.39	1.2183e-06	2.54		
64	1.9913e-06	2.34	2.1130e-07	2.53		
128	4.5245e-07	2.14	4.5142e-08	2.23		

### 4.2. The energy dissipation and mass conservation

To show that the numerical scheme satisfies the discrete energy law and mass conservation, the Coulomb-driven flow in a cavity is considered. The terminal time is set to be  $T = 2$ . We take the steric interaction coefficient matrix  $W = \begin{pmatrix} 2 & 0 \\ 0 & 2 \end{pmatrix}$ . The parameters are set as  $\lambda = 0.2$ ,  $Pe = 50$ ,  $Re = 1$ ,  $Co = 0.6$ ,  $k = 0.2$ ,



$\mu_0 = 1.5, \mu_\infty = 0.5, \lambda_1 = 0.1$ . The spatial mesh size is chosen to be  $h = \frac{\sqrt{2}}{40}$ . The initial conditions are taken to be

$$\begin{aligned} c_{p0} &= 12 + 10 \cos(\pi x) \cos(\pi y), \\ c_{n0} &= 12 - 10 \cos(\pi x) \cos(\pi y), \\ \mathbf{u}_0 &= (0, 0), \end{aligned} \tag{41}$$

where the initial condition for the electric potential satisfies  $\int_{K_h} V d\mathbf{x} = 0$ . In Fig. 1, we present the time evolution of the discrete total energy and variable  $\xi$  for different time step  $\Delta t$ , one can see that the numerical scheme dissipates the total energy which is consistent with the theoretical analysis. Fig. 2 depicts the values of the auxiliary variable  $\xi$  with diverse time step sizes. One can see that the numerical solutions of the variable is approximately equal to 1. Fig. 3 plots time evolution of the discrete masses  $\int_{\Omega} c_p d\mathbf{x}$  and  $\int_{\Omega} c_n d\mathbf{x}$ , which demonstrates the mass conservation property of the scheme.

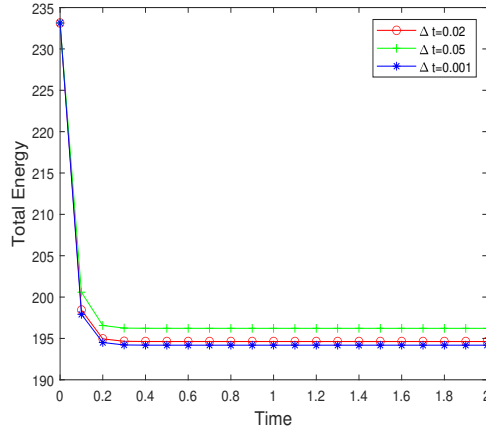


Fig. 1: Time evolution of the discrete total energy .

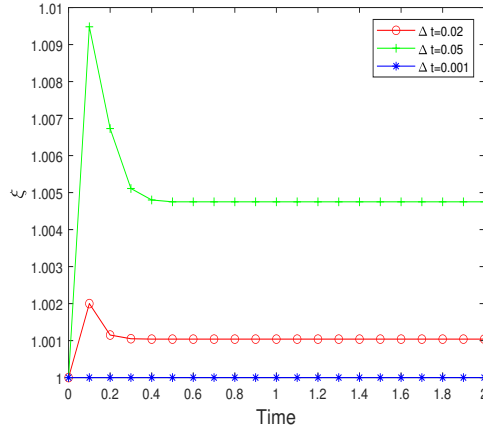


Fig. 2: Time evolution of the auxiliary variable  $\xi$ .

#### 4.3. Steric effect

To study the effect of steric interactions on the ion distribution, we take the steric interaction coefficient matrices  $W = \begin{pmatrix} 0 & 0 \\ 0 & 0 \end{pmatrix}, \begin{pmatrix} 4 & 1 \\ 1 & 4 \end{pmatrix}, \begin{pmatrix} 8 & 1 \\ 1 & 8 \end{pmatrix}, \begin{pmatrix} 8 & 4 \\ 4 & 8 \end{pmatrix}, \begin{pmatrix} 8 & 7 \\ 7 & 8 \end{pmatrix}$ . The initial conditions are given as

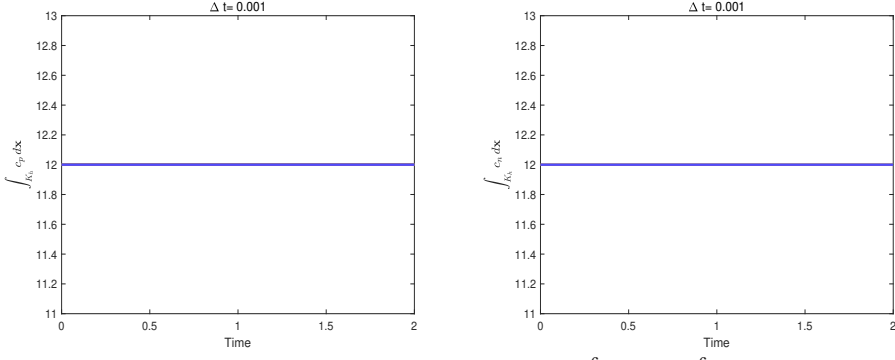


Fig. 3: Time evolution of the discrete masses  $\int_{\Omega} c_p dx$  and  $\int_{\Omega} c_n dx$ .

follows

$$\begin{aligned} \mathbf{u}_0 &= (0, 0), \\ c_{p0} &= 10^{-6} + (1 - 10^{-6}) \cdot H(x) \cdot H_1(y), \\ c_{n0} &= 10^{-6} + (1 - 10^{-6}) \cdot H(x) \cdot H_2(y), \end{aligned}$$

where

$$\begin{aligned} H(x) &= \frac{1}{2} \left[ 1 + \tanh\left(\frac{x - 0.75}{0.04}\right) \right], \\ H_1(y) &= \frac{1}{2} \left[ 1 + \tanh\left(\frac{y - 0.55}{0.04}\right) \right], \\ H_2(y) &= \frac{1}{2} \left[ 1 + \tanh\left(\frac{0.45 - y}{0.04}\right) \right]. \end{aligned}$$

We set the computed domain to be  $\Omega = [0, 1]^2$ . In the computations, the parameters are set as  $\lambda = 0.1$ ,  $Pe = 50$ ,  $Re = 5$ ,  $Co = 5$ ,  $k = 0.5$ ,  $\mu_0 = 1.0$ ,  $\mu_\infty = 0.5$ ,  $\lambda_1 = 1$ ,  $\Delta t = 0.001$ ,  $h = \frac{\sqrt{2}}{40}$ . The snapshots of  $c_p$ ,  $c_n$  and  $V$  at  $t = 0.002$ ,  $t = 0.1$  and  $t = 1$  for various  $W$  are shown in Fig. 4 - Fig. 8, respectively. With increasing diagonal entries in  $W$ , enhanced self steric interactions among same species of ions drives spatial dispersion, resulting in both broader distribution and reduced peak concentration as ions maximize the distances between same species of ions. As the off-diagonal entries in  $W$  increases, stronger cross steric interactions between different species of ions cause the peak concentration to increase and the non-zero concentration region to shrink.

#### 4.4. Effects of exponent $k$

In this test, we consider the effects of exponent  $k$  on the velocity field. We set the computed domain to be  $\Omega = [0, 1]^2$ . The initial and boundary conditions are

$$\begin{aligned} c_{p0} &= 1 + 10^{-6} - \tanh(100((x - 0.4)^2 + (y - 0.4)^2 - (0.05)^2)), \\ c_{n0} &= 1 + 10^{-6} - \tanh(100((x - 0.6)^2 + (y - 0.6)^2 - (0.05)^2)), \quad \mathbf{u}_0 = (0, 0), \\ x = 0 : \quad V &= 1, \quad \frac{\partial c_p}{\partial \mathbf{n}} = \frac{\partial c_n}{\partial \mathbf{n}} = 0, \quad u = 0, \quad v = 0, \\ x = 1 : \quad V &= 0, \quad \frac{\partial c_p}{\partial \mathbf{n}} = \frac{\partial c_n}{\partial \mathbf{n}} = 0, \quad u = 0, \quad v = 0, \\ y = 0, 1 : \quad \frac{\partial V}{\partial \mathbf{n}} &= \frac{\partial c_p}{\partial \mathbf{n}} = \frac{\partial c_n}{\partial \mathbf{n}} = 0, \quad u = 0, \quad v = 0. \end{aligned} \tag{42}$$

The parameters are set as  $\lambda = 0.1$ ,  $Pe = 50$ ,  $Re = 50$ ,  $Co = 100$ ,  $\mu_0 = 1.0$ ,  $\mu_\infty = 0.1$ ,  $\lambda_1 = 0.1$ ,  $\Delta t = 0.001$  and  $h = \frac{\sqrt{2}}{60}$ . The time evolution of the streamlines are given in Fig. 9. Across all  $k$  values, a single vortex was observed at  $t = 5$ , with its shape distinctly influenced by the shear behavior. For  $k < 1$ , indicative of shear thinning, the vortex core appeared flattened along the flow direction. At  $k = 1$ , representing Newtonian

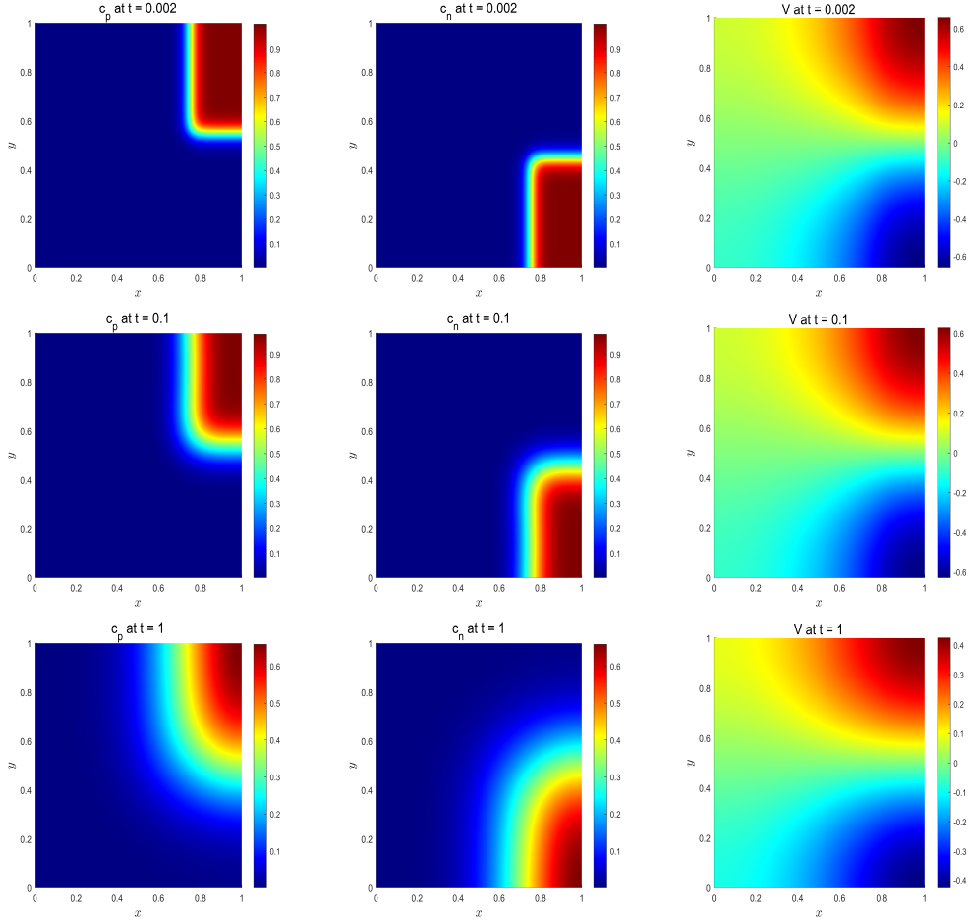


Fig. 4: Snapshots of  $c_p$ ,  $c_n$  and  $V$  for  $\omega_{11} = \omega_{22} = 0$ ,  $\omega_{12} = \omega_{21} = 0$  at  $t = 0.002$ ,  $t = 0.1$  and  $t = 1$ .

behavior, the vortex core was less flattened. Conversely, for  $k > 1$ , which denotes shear thickening, the vortex core was more rounded and oriented more vertically. Fig. 10 shows the snapshots of  $c_p - c_n$  for  $t = 0.005, 0.075, 0.1, 0.2, 0.3, 5$  at  $k = 0.4$ . At the end of the computation, the fluid becomes almost electron-neutral.

## 5. Conclusions

In this paper, to explore the impact of steric effect on ion transport in non-Newtonian fluid, we have developed a linear, decoupled, second-order accurate in time and structure-preserving scheme for Carreau fluid equations coupled with steric PNP model. The novelty of the proposed scheme is based on the decoupling technique by introducing a nonlocal auxiliary variable with respect to the free energy of steric PNP equations and splitting method for the fluid equation. Moreover, at each time step, we only need to solve several linear equations. The fully discrete numerical scheme has proved to be energy stable, and preserve positivity and mass conservation of the ion concentration. The accuracy and effectiveness of the scheme are verified by numerical experiments.

## References

- [1] Junghoon Lee and Chang-Jin Kim. Surface-tension-driven microactuation based on continuous electrowetting. *Journal of Microelectromechanical Systems*, 9(2):171–180, 2000.

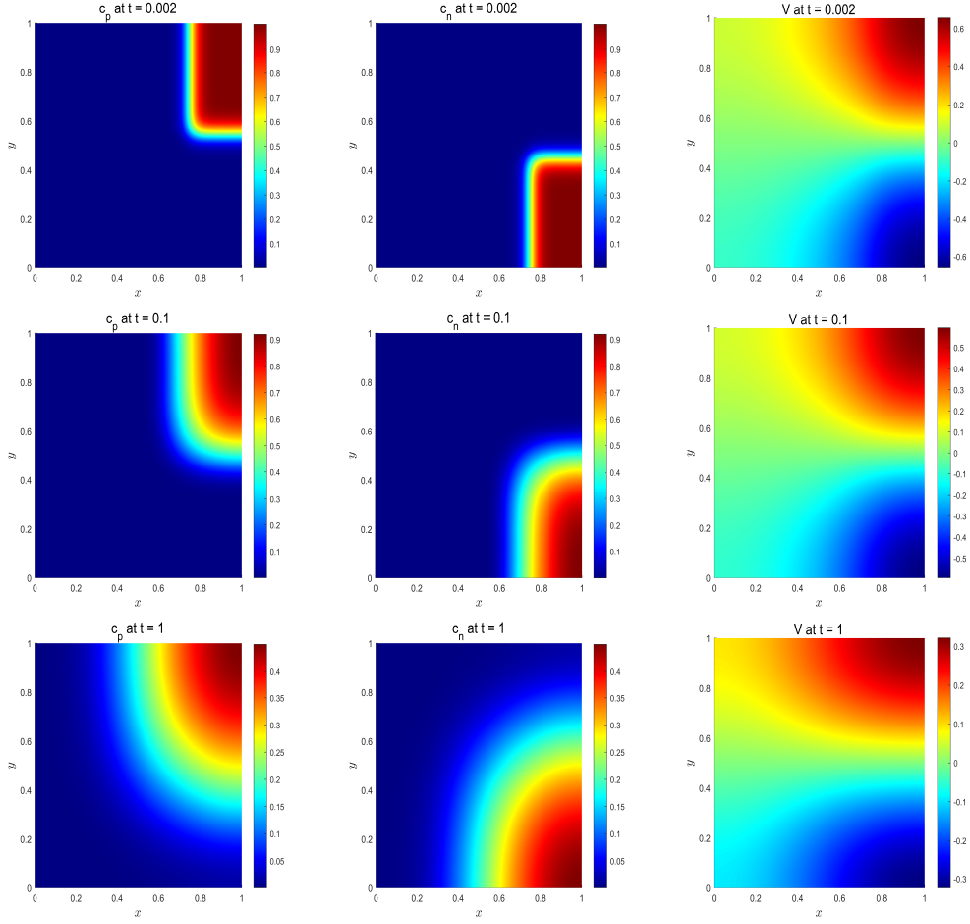


Fig. 5: Snapshots of  $c_p$ ,  $c_n$  and  $V$  for  $\omega_{11} = \omega_{22} = 4$ ,  $\omega_{12} = \omega_{21} = 1$  at  $t = 0.002$ ,  $t = 0.1$  and  $t = 1$ .

- [2] Sandip Ghosal. Electrokinetic flow and dispersion in capillary electrophoresis. *Annu. Rev. Fluid Mech.*, 38(1):309–338, 2006.
- [3] Christoffer P Nielsen and Henrik Bruus. Concentration polarization, surface currents, and bulk advection in a microchannel. *Physical Review E*, 90(4):043020, 2014.
- [4] Hae-Won Choi and Marius Paraschivoiu. Advanced hybrid-flux approach for output bounds of electro-osmotic flows: adaptive refinement and direct equilibrating strategies. *Microfluidics and Nanofluidics*, 2(2):154–170, 2006.
- [5] Victor V Nikonenko, Anna V Kovalenko, Mahamet K Urtenov, Natalia D Pismenskaya, Jongyoon Han, Philippe Sistat, and Gérald Pourcelly. Desalination at overlimiting currents: State-of-the-art and perspectives. *Desalination*, 342:85–106, 2014.
- [6] Chien-Hsiung Tsai, Ruey-Jen Yang, Chang-Hsien Tai, and Lung-Ming Fu. Numerical simulation of electrokinetic injection techniques in capillary electrophoresis microchips. *electrophoresis*, 26(3):674–686, 2005.
- [7] Yandong Hu, Jacky SH Lee, Carsten Werner, and Dongqing Li. Electrokinetically controlled concentration gradients in micro-chambers in microfluidic systems. *Microfluidics and Nanofluidics*, 2(2):141–153, 2006.
- [8] Herbert Gajewski and Konrad Gröger. On the basic equations for carrier transport in semiconductors. *Journal of mathematical analysis and applications*, 113(1):12–35, 1986.

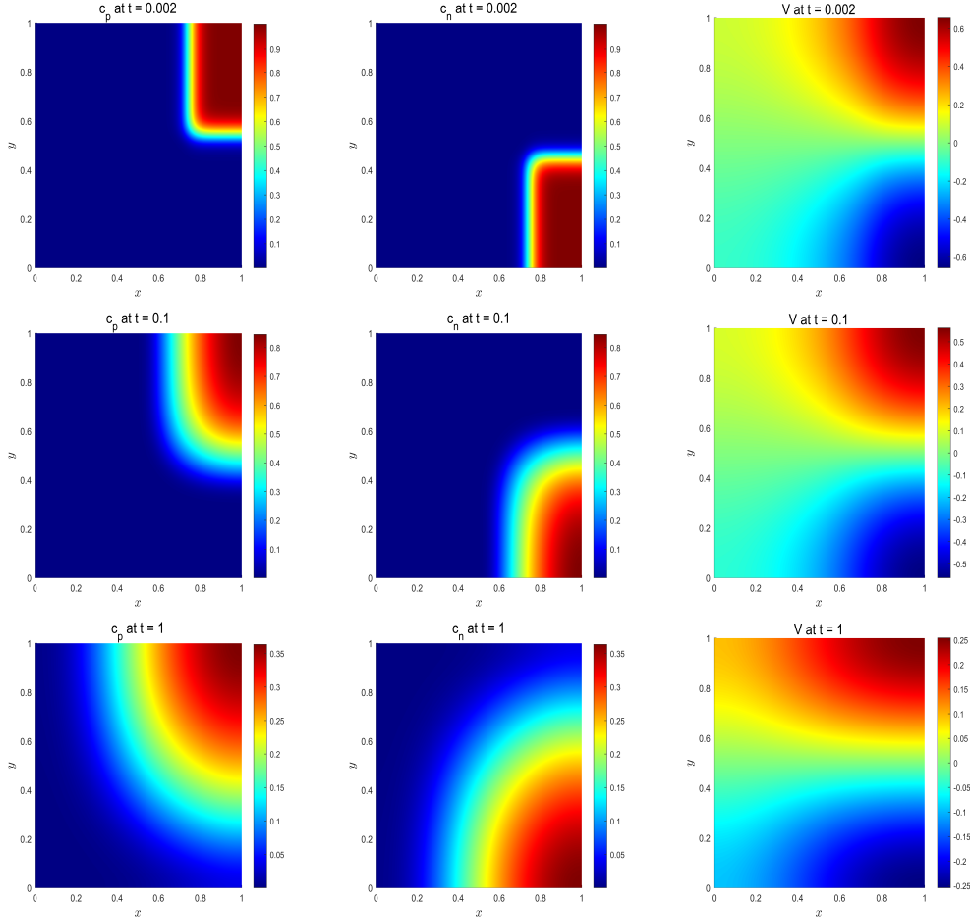


Fig. 6: Snapshots of  $c_p$ ,  $c_n$  and  $V$  for  $\omega_{11} = \omega_{22} = 8$ ,  $\omega_{12} = \omega_{21} = 1$  at  $t = 0.002$ ,  $t = 0.1$  and  $t = 1$ .

- [9] Franco Brezzi, Luisa Donatella Marini, and Paola Pietra. Numerical simulation of semiconductor devices. *Computer methods in applied mechanics and engineering*, 75(1-3):493–514, 1989.
- [10] Bob Eisenberg and Weishi Liu. Poisson-nernst-planck systems for ion channels with permanent charges. *SIAM journal on mathematical analysis*, 38(6):1932–1966, 2007.
- [11] Benzhuo Lu, Michael J Holst, J Andrew McCammon, and Yongcheng Zhou. Poisson–nernst–planck equations for simulating biomolecular diffusion–reaction processes i: Finite element solutions. *Journal of computational physics*, 229(19):6979–6994, 2010.
- [12] Guo-Wei Wei, Qiong Zheng, Zhan Chen, and Kelin Xia. Variational multiscale models for charge transport. *siam REVIEW*, 54(4):699–754, 2012.
- [13] Tzyy-Leng Horng, Tai-Chia Lin, Chun Liu, and Bob Eisenberg. Pnp equations with steric effects: a model of ion flow through channels. *The journal of physical chemistry. B*, 116 37:11422–41, 2012.
- [14] Mustafa Kili, Martin Z. Bazant, and Armand Ajdari. Steric effects in the dynamics of electrolytes at large applied voltages. ii. modified poisson-nernst-planck equations. *Physical review. E, Statistical, nonlinear, and soft matter physics*, 75 2 Pt 1:021503, 2006.
- [15] Benzhuo Lu and Y. C. Zhou. Poisson-nernst-planck equations for simulating biomolecular diffusion-reaction processes ii: size effects on ionic distributions and diffusion-reaction rates. *Biophysical journal*, 100 10:2475–85, 2011.

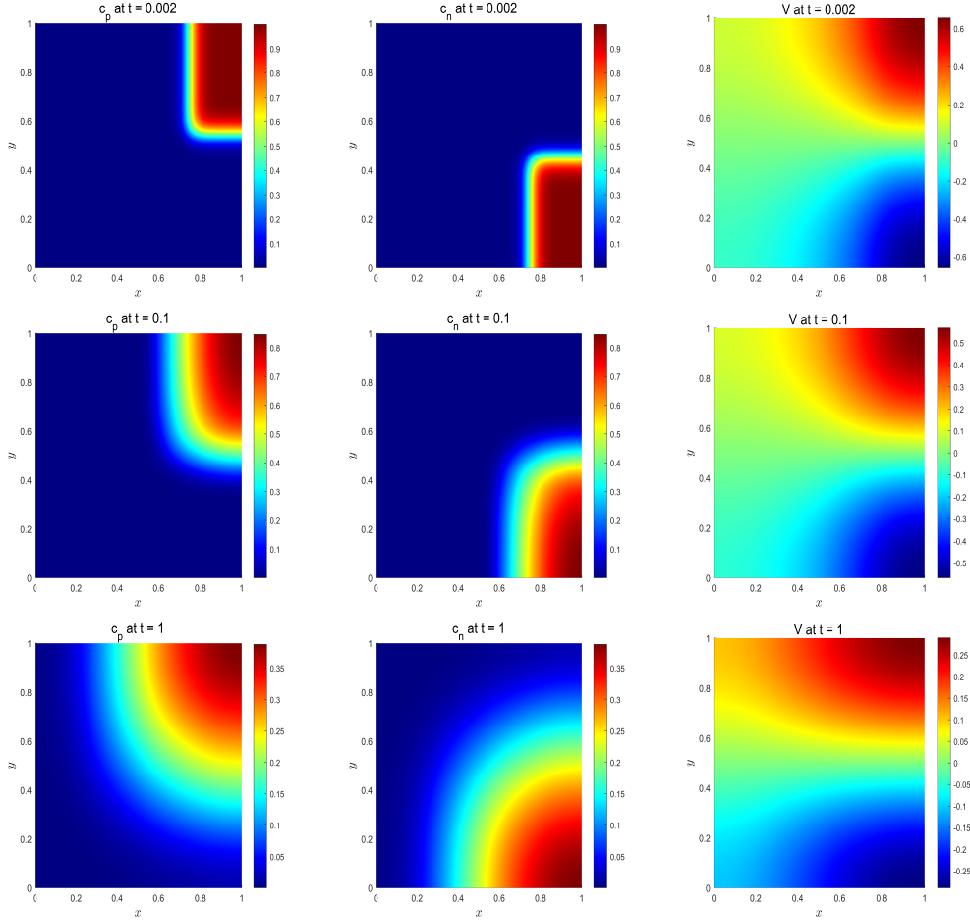


Fig. 7: Snapshots of  $c_p$ ,  $c_n$  and  $V$  for  $\omega_{11} = \omega_{22} = 8$ ,  $\omega_{12} = \omega_{21} = 4$  at  $t = 0.002$ ,  $t = 0.1$  and  $t = 1$ .

- [16] Farjana Siddiqua, Zhongming Wang, and Shenggao Zhou. A modified poisson–nernst–planck model with excluded volume effect: Theory and numerical implementation. *arXiv: Statistical Mechanics*, 2017.
- [17] Tai-Chia Lin and Bob Eisenberg. A new approach to the lennard-jones potential and a new model: Pnp-steric equations. *Communications in Mathematical Sciences*, 12(1):149–173, 2013.
- [18] Jie Ding, Zhongming Wang, and Shenggao Zhou. Positivity preserving finite difference methods for poisson–nernst–planck equations with steric interactions: Application to slit-shaped nanopore conductance. *J. Comput. Phys.*, 397, 2019.
- [19] Georg Bauer, Volker Gravemeier, and Wolfgang A Wall. A stabilized finite element method for the numerical simulation of multi-ion transport in electrochemical systems. *Computer methods in applied mechanics and engineering*, 223:199–210, 2012.
- [20] Markus Schmuck. Analysis of the navier-stokes–nernst–planck–poisson system. *Mathematical Models and Methods in Applied Sciences*, 19(06):993–1014, 2009.
- [21] Maximilian Metti, Jinchao Xu, and Chun Liu. Energetically stable discretizations for charge transport and electrokinetic models. *J. Comput. Phys.*, 306:1–18, 2016.
- [22] Gaute Linga, Asger Bolet, and Joachim Mathiesen. Transient electrohydrodynamic flow with concentration-dependent fluid properties: modelling and energy-stable numerical schemes. *Journal of Computational Physics*, 412:109430, 2020.

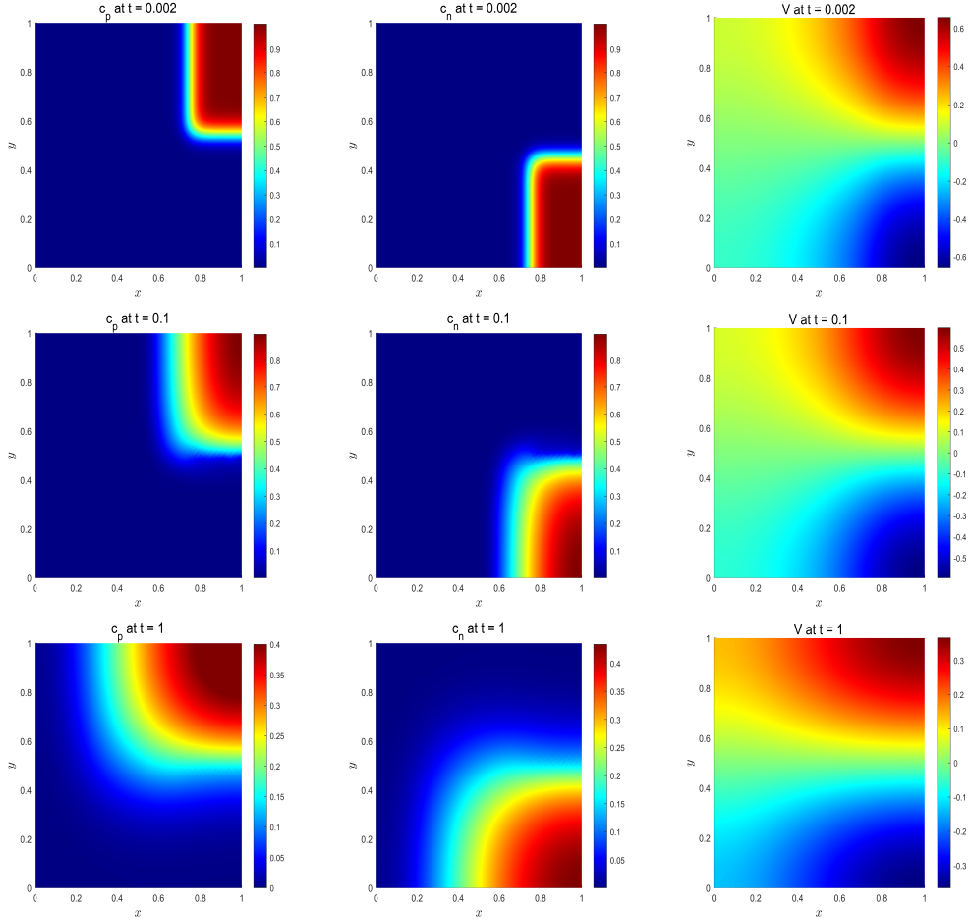


Fig. 8: Snapshots of  $c_p$ ,  $c_n$  and  $V$  for  $\omega_{11} = \omega_{22} = 8$ ,  $\omega_{12} = \omega_{21} = 7$  at  $t = 0.002$ ,  $t = 0.1$  and  $t = 1$ .

- [23] Mingyang Pan, Sifu Liu, Wenxing Zhu, Fengyu Jiao, and Dongdong He. A linear, second-order accurate, positivity-preserving and unconditionally energy stable scheme for the navier–stokes–poisson–nernst–planck system. *Communications in Nonlinear Science and Numerical Simulation*, 131:107873, 2024.
- [24] Shu Wang, Limin Jiang, and Chundi Liu. Quasi-neutral limit and the boundary layer problem of planck–nernst–poisson–navier–stokes equations for electro–hydrodynamics. *Journal of Differential Equations*, 267(6):3475–3523, 2019.
- [25] Yong Wang, Chun Liu, and Zhong Tan. A generalized poisson–nernst–planck–navier–stokes model on the fluid with the crowded charged particles: Derivation and its well-posedness. *SIAM Journal on Mathematical Analysis*, 48(5):3191–3235, 2016.
- [26] Shixin Xu, Ping Sheng, and Chun Liu. An energetic variational approach for ion transport. *Communications in Mathematical Sciences*, 12(4):779–789, 2014.
- [27] Minghao Li and Zhenzhen Li. Error estimates for the finite element method of the navier–stokes–poisson–nernst–planck equations. *Applied Numerical Mathematics*, 197:186–209, 2024.
- [28] Pierre J Carreau. Rheological equations from molecular network theories. *Transactions of the Society of Rheology*, 16(1):99–127, 1972.
- [29] IL Animasaun and I Pop. Numerical exploration of a non-newtonian carreau fluid flow driven by



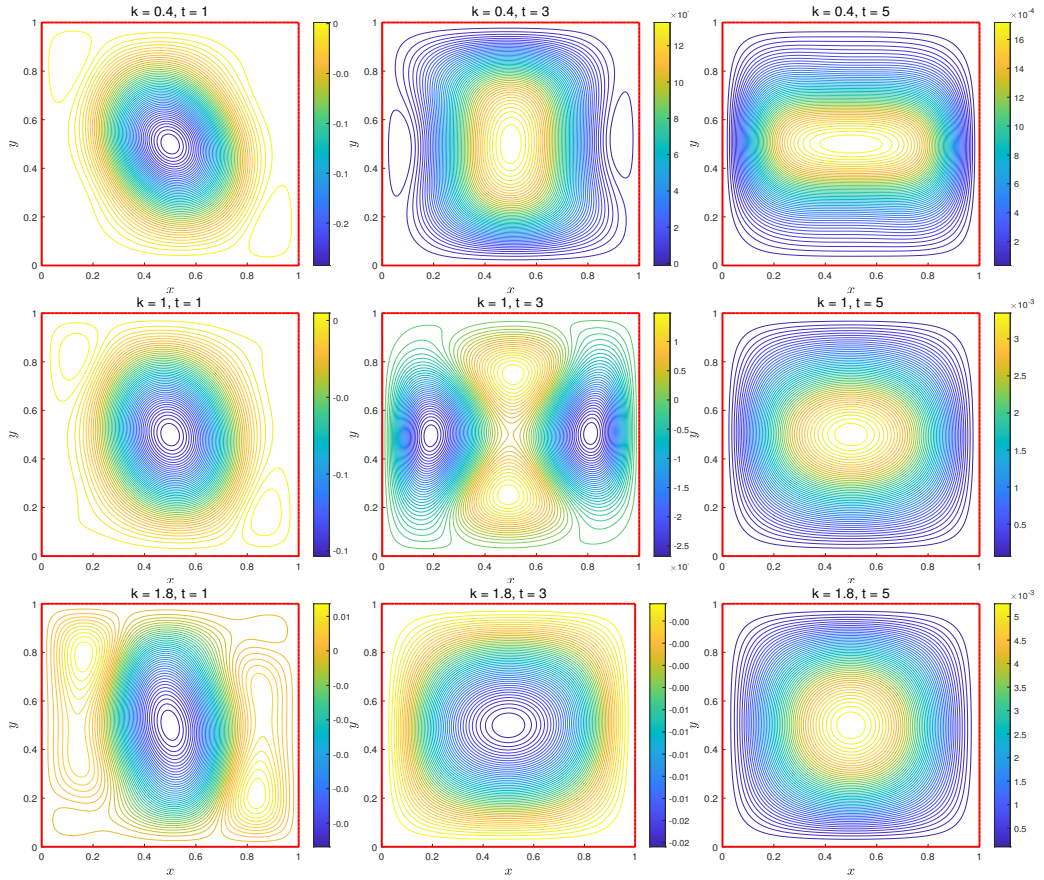


Fig. 9: Time evolution of streamlines for  $k = 0.4$ ,  $k = 1$  and  $k = 1.8$ .

catalytic surface reactions on an upper horizontal surface of a paraboloid of revolution, buoyancy and stretching at the free stream. *Alexandria Engineering Journal*, 56(4):647–658, 2017.

- [30] M Waqas, M Ijaz Khan, T Hayat, and A Alsaedi. Numerical simulation for magneto carreau nanofluid model with thermal radiation: a revised model. *Computer Methods in Applied Mechanics and Engineering*, 324:640–653, 2017.
- [31] P Sivakumar, Ram Prakash Bharti, and RP Chhabra. Effect of power-law index on critical parameters for power-law flow across an unconfined circular cylinder. *Chemical Engineering Science*, 61(18):6035–6046, 2006.
- [32] Wenxing Zhu, Mingyang Pan, Qinghe Wang, Fengyu Jiao, and Dongdong He. Decoupled second-order energy stable scheme for an electrohydrodynamic model with variable electrical conductivity. *Journal of Computational and Applied Mathematics*, 438:115530, 2024.
- [33] J-L Guermond and Luigi Quartapelle. A projection fem for variable density incompressible flows. *Journal of Computational Physics*, 165(1):167–188, 2000.
- [34] Rolf Rannacher. On chorin’s projection method for the incompressible navier-stokes equations. In *The Navier-Stokes Equations II—Theory and Numerical Methods: Proceedings of a Conference held in Oberwolfach, Germany, August 18–24, 1991*, pages 167–183. Springer, 2006.
- [35] Jean-Luc Guermond, Peter Mineev, and Jie Shen. An overview of projection methods for incompressible flows. *Computer methods in applied mechanics and engineering*, 195(44-47):6011–6045, 2006.



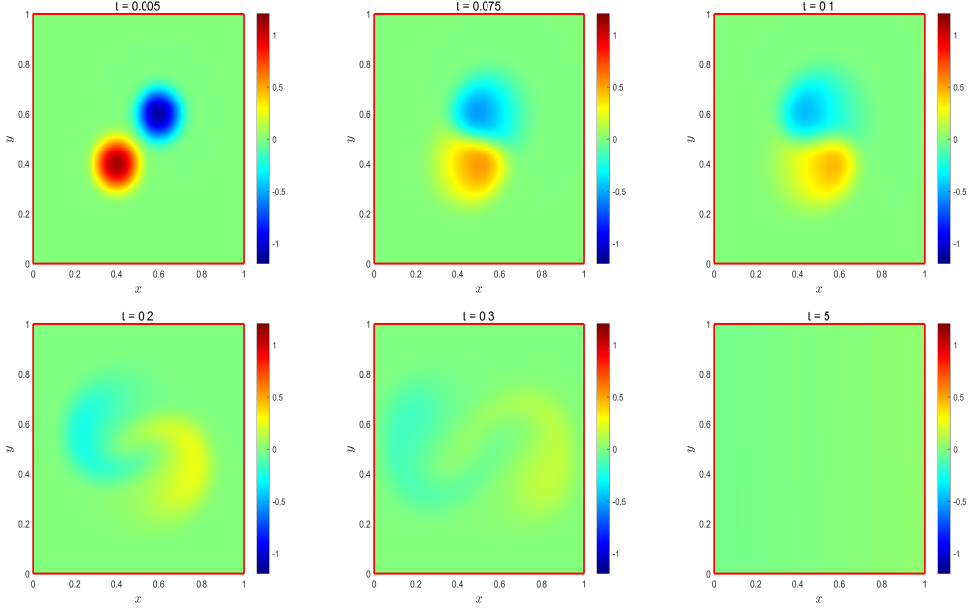


Fig. 10: Snapshots of  $c_p - c_n$  for  $t = 0.005, 0.075, 0.1, 0.2, 0.3, 0.5$  at  $k = 0.4$ .

- [36] J-L Guermond and Abner Salgado. A splitting method for incompressible flows with variable density based on a pressure poisson equation. *Journal of Computational Physics*, 228(8):2834–2846, 2009.
- [37] Andreas Prohl and Markus Schmuck. Convergent discretizations for the nernst–planck–poisson system. *Numerische Mathematik*, 111(4):591–630, 2009.
- [38] Allen Flavell, Michael Machen, Bob Eisenberg, Julianne Kabre, Chun Liu, and Xiaofan Li. A conservative finite difference scheme for poisson–nernst–planck equations. *Journal of Computational Electronics*, 13(1):235–249, 2014.
- [39] Huadong Gao and Dongdong He. Linearized conservative finite element methods for the nernst–planck–poisson equations. *Journal of Scientific Computing*, 72(3):1269–1289, 2017.
- [40] Dongdong He and Kejia Pan. An energy preserving finite difference scheme for the poisson–nernst–planck system. *Applied Mathematics and Computation*, 287:214–223, 2016.
- [41] Jie Shen, Jie Xu, and Jiang Yang. The scalar auxiliary variable (sav) approach for gradient flows. *Journal of Computational Physics*, 353:407–416, 2018.
- [42] Dongdong He, Kejia Pan, and Xiaoqiang Yue. A positivity preserving and free energy dissipative difference scheme for the poisson–nernst–planck system. *Journal of Scientific Computing*, 81(1):436–458, 2019.
- [43] Jingwei Hu and Xiaodong Huang. A fully discrete positivity-preserving and energy-dissipative finite difference scheme for poisson–nernst–planck equations. *Numerische Mathematik*, 145(1):77–115, 2020.
- [44] Jie Shen and Jie Xu. Unconditionally positivity preserving and energy dissipative schemes for poisson–nernst–planck equations. *Numerische Mathematik*, 148(3):671–697, 2021.
- [45] Andreas Prohl and Markus Schmuck. Convergent finite element discretizations of the navier–stokes–nernst–planck–poisson system. *Mathematical Modelling and Numerical Analysis*, 44:531–571, 2010.
- [46] Mingyan He and Pengtao Sun. Mixed finite element analysis for the poisson–nernst–planck/stokes coupling. *Journal of Computational and Applied Mathematics*, 341:61–79, 2018.

- [47] Xiaolan Zhou and Chuanju Xu. Efficient time-stepping schemes for the navier-stokes-nernst-planck-poisson equations. *Computer Physics Communications*, 289:108763, 2023.
- [48] Jie Shen, Jie Xu, and Jiang Yang. A new class of efficient and robust energy stable schemes for gradient flows. *SIAM Review*, 61(3):474–506, 2019.
- [49] Vivette Girault and Pierre-Arnaud Raviart. An analysis of a mixed finite element method for the navier-stokes equations. *Numerische Mathematik*, 33(3):235–271, 1979.
- [50] Frédéric Hecht. New development in FreeFem++. *J. Numer. Math.*, 20:251–266, 2012.